Chemical Science

ROYAL SOCIETY OF CHEMISTRY

EDGE ARTICLE

View Article Online
View Journal | View Issue

Cite this: *Chem. Sci.*, 2024, **15**, 10592

All publication charges for this article have been paid for by the Royal Society of Chemistry

Visible-light-induced direct C–H alkylation of polycyclic aromatic hydrocarbons with alkylsulfones†

Motoo Ohtsuka,‡[a] Koushik Ghosh,‡[a] Jacky C.-H. Yim,‡[a] Hikaru Sotome,[b]* Tsubasa Okamoto,[cd] Kayo Suda,[e] Yasuhiro Kobori,[cd]* Daisuke Yokogawa,[e]* Hiroshi Miyasaka,[b]* Cathleen M. Crudden[afg]* and Masakazu Nambo[ah]*

Received 18th April 2024
Accepted 25th May 2024

DOI: 10.1039/d4sc02577f

rsc.li/chemical-science

Polycyclic aromatic hydrocarbons (PAHs) are fragments of graphene that have attracted considerable attention as a new class of carbon-based materials. The functionalization of edge positions in PAHs is important to enable the modulation of physical and chemical properties essential for various applications. However, straightforward methods that combine functional group tolerance and regioselectivity remain sought after. Here we report a photochemical approach for the direct alkylation of carbon–hydrogen bonds in PAHs that takes place in a regiospecific manner, an outcome that has never been achieved in related thermal reactions. A reaction mechanism involving a single electron transfer process from photo-excited PAHs to sulfones, and a rationale for the origin of regioselectivity are proposed on the basis of spectroscopic analyses and theoretical calculations.

Introduction

The synthesis of well-defined aromatic compounds has been of central importance in organic chemistry since the very beginning of the field.[1–3] In modern times, aromatic substructures are found in virtually all pharmaceutical compounds and are key components of many polymers and materials.[4–6] Among aromatic compounds, polycyclic aromatic hydrocarbons (PAHs) have attracted much attention both as fragments of graphene and also as interesting materials in their own right (Fig. 1a). Functionalized PAHs have already shown promise in organic electronic devices, bioimaging, sensing, and gene delivery.[7,8] In recent years, several bottom-up approaches have been developed that enable the preparation of new atomically precise PAHs, including systems with embedded heteroatoms and rings of varying sizes.[9,10] To explore the functions of these new PAHs, methods to modify edge sites are crucial because they enhance solubility and processability, and enable the tuning of intermolecular interactions and electronic properties – all critical factors in materials applications.[11,12] However, the introduction of functionality into PAHs often requires harsh reaction conditions, which limit applicable functional groups or require long synthetic sequences to introduce desired substituents regioselectively. Therefore, the development of straightforward methods for site-selective functionalization of carbon–hydrogen (C–H) bonds in PAHs is essential for the field to progress.

Among direct methods to introduce functional groups onto PAHs,[13–15] Friedel–Crafts reactions have been the most widely employed (Fig. 1b).[16] As expected from this classical reaction, strong acids are needed,[17,18] resulting in low functional group compatibility. Moreover, groups that can be introduced are limited to very simple alkyl substituents. Accurate control of the regioselectivity is also a significant challenge for Friedel–Crafts reactions on PAHs. For pyrene, electrophilic aromatic substitution generally occurs at the C1, C3, C6, and C8 positions, whereas bulky tertiary alkyl groups are installed at the C2 and

[a]*Institute of Transformative Bio-Molecules (WPI-ITbM), Nagoya University, Chikusa, Nagoya, Aichi, 464-8601, Japan. E-mail: cruddenc@chem.queensu.ca; nambo.masakazu.p3@f.mail.nagoya-u.ac.jp*

[b]*Division of Frontier Materials Science and Centre for Advanced Interdisciplinary Research, Graduate School of Engineering Science, Osaka University, 1-3 Machikaneyama, Toyonaka, Osaka 560-8531, Japan. E-mail: sotome@laser.chem.es.osaka-u.ac.jp*

[c]*Molecular Photoscience Research Center, Kobe University, 1-1 Rokkodai-cho, Nada-ku, Kobe 657-8501, Japan. E-mail: ykobori@kitty.kobe-u.ac.jp*

[d]*Department of Chemistry, Graduate School of Science, Kobe University, 1-1, Rokkodai-cho, Nada-ku, Kobe 657-8501, Japan*

[e]*Graduate School of Arts and Sciences, The University of Tokyo, Komaba, Meguro-ku, Tokyo, 153-8902, Japan. E-mail: c-d.yokogawa@g.ecc.u-tokyo.ac.jp*

[f]*Department of Chemistry, Queen's University, Chernoff Hall, Kingston, Ontario K7L 3N6, Canada*

[g]*Carbon to Metal Coating Institute, Queen's University, Kingston, Ontario, K7L 3N6, Canada*

[h]*Department of Chemistry, Graduate School of Science, Nagoya University, Furo, Chikusa, Nagoya, Aichi, 464-8601, Japan*

† Electronic supplementary information (ESI) available. CCDC 2312745. For ESI and crystallographic data in CIF or other electronic format see DOI: https://doi.org/10.1039/d4sc02577f

‡ These authors contributed equally.

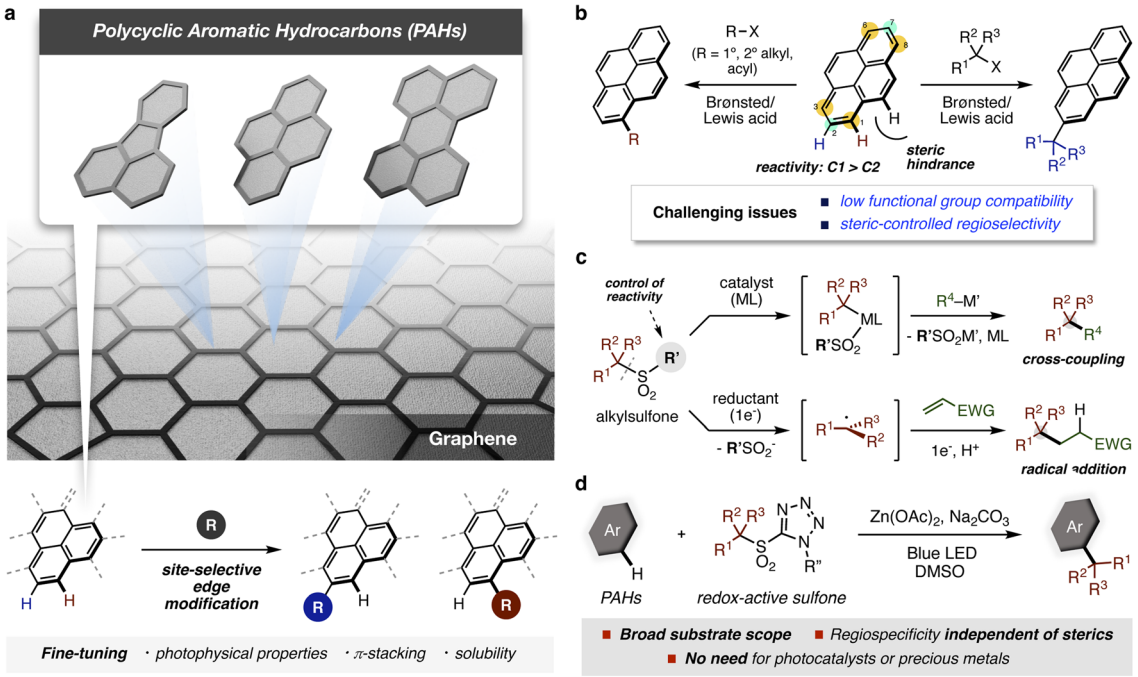

Fig. 1 Edge modification of polycyclic aromatic hydrocarbons (PAHs): (a) site-selective functionalizations of PAHs for tuning molecular functions. (b) Regioselectivity in Friedel–Crafts reaction of pyrene (X = halides or OH). (c) Desulfonylative transformations of sulfones. (d) This work: visible-light-induced regiospecific C–H alkylation of PAHs with redox-active alkyl sulfones.

C7 positions. Steric effects also control the regioselectivity of Ir-catalyzed C–H borylations, which have been reported by the Marder group to introduce synthetically useful boryl groups.[19] To date, there is only one example of *tert*-butylation of pyrene at the C1 position under electrochemical conditions, which includes hydroalkylated pyrenes as side products.[20] The regioselectivity in classical thermal functionalizations of PAHs has therefore depended on the bulkiness of substituents for control, illustrating the need for new synthetic approaches to prepare structurally diverse PAH derivatives.

Over the past few decades, sulfones have emerged as versatile, readily available building blocks owing to their bench stability and functional group compatibility (Fig. 1c).[21] Compared with (pseudo)halides, the sulfonyl group is less reactive, and thus has received less attention as a leaving group in organic synthesis. However, recent results have shown that subtle changes to the non-reactive portion can result in versatile reactivity in transition-metal catalyzed reactions.[22,23] Furthermore, reductive activation of alkyl sulfones through single electron transfer (SET) has enabled radical functionalization reactions under mild conditions.[24–28]

During our investigations into radical generation from sulfones using PAHs as photocatalysts, we observed the formation of alkylated PAHs. Building on this observation, we envisioned that a photo-induced process might provide a powerful solution to the issue of regioselective functionalization of PAHs without resorting to photocatalysts or precious metals. Herein, we report a simple photochemical method for the direct C–H alkylation of PAHs with redox-active alkylsulfones in a regiospecific manner never before achieved under thermal conditions (Fig. 1d). This method provides a variety of alkylated PAHs bearing useful functional groups under mild reaction conditions, increasing the potential utility for PAH-based organic materials. A reaction mechanism involving a SET and a regiospecific carbon–carbon bond forming processes is proposed based on spectroscopic analyses and theoretical calculations.

Results and discussion

We began our investigation of the direct C–H alkylation of 2-*tert*-butylpyrene **1a** as a model PAH. A blue light-emitting diode (LED, 456 nm) was employed for irradiation. In early experiments using 1,1-dimethylpropyl *N*-phenyltetrazolyl sulfone **2a** as the alkylating agent and DMSO as solvent, Na_2CO_3 was found to be the optimal base (see ESI, Table S1†), affording mono-alkylated- (**8a**) and di-alkylated products (**8aa**) in 30% and 5% yields, respectively. Surprisingly, the alkylation occurred exclusively at the sterically-hindered C6 and C8 positions, in contrast with Friedel–Crafts alkylation conditions, which yield the C7-alkylated product.

The wavelength dependence of LEDs in C–H alkylation was investigated next (Fig. 2a). The yields of both products depended on the wavelength of light, with lower yields obtained at shorter wavelengths. When the progress of the reaction was monitored by HPLC, rapid decomposition of sulfone **2a** was observed using a UV LED (370 nm), suggesting that sulfone stability suffers under UV light irradiation and that visible light in the blue region of the spectrum is optimal (see ESI, Fig. S4†).

To improve the reaction efficiency, the aryl substituent on the tetrazolyl group was modified (Fig. 2b). The electron-deficient 4-trifluoromethylphenyl group (**3a**) showed similar

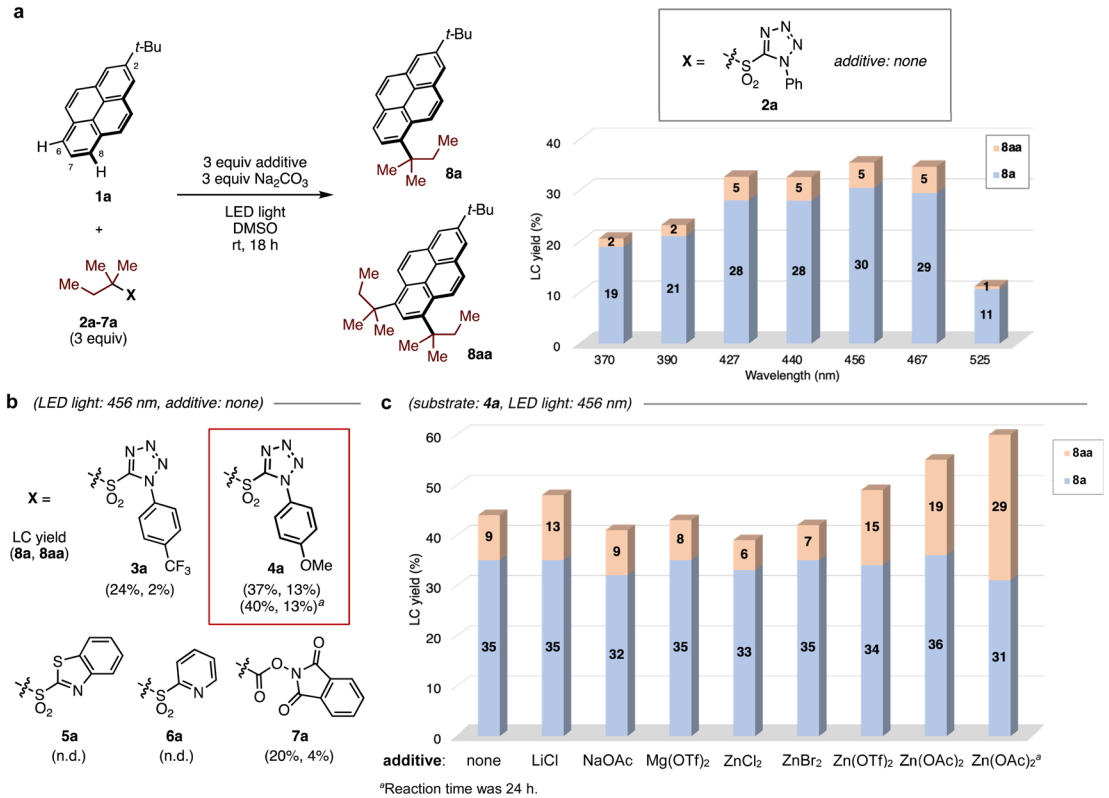

Fig. 2 Optimization of reaction conditions in visible-light-induced C–H alkylation: (a) LED wavelength dependence in the reaction of 2-*tert*-butylpyrene **1a** with alkylating agents. Yields were determined by high performance liquid chromatography (LC) of crude mixture using biphenyl as an internal standard. (b) Effect of substituents (X) in redox-active substrates. (c) Effect of additives when **4a** was used.

reactivity, and the electron-rich 4-methoxyphenyl group (**4a**) slightly increased the yield of **8aa**. Notably, the replacement of tetrazolyl group with other substituents such as 2-benzothiazolyl (**5a**) and 2-pyridyl (**6a**) groups shut down the reaction. A redox-active *N*-hydroxyphthalimide ester **7a**, which is widely employed for radical transformations,[29] gave low yields of both products. Further optimization was attempted by screening of various additives (Fig. 2c, see ESI, Table S3†). While metal salts including Li and Mg salts were not effective, the addition of $Zn(OAc)_2$ led to increased yields of **8aa**. Prolonging the reaction time increased the combined yield of **8a**/**8aa** to 60%. However, if **8a** alone is the desired product, the reaction without additive provides similar yields of this product, with only 9% double alkylation. The role of Zn salt is not clear, but the degradation of alkyl sulfone appeared to be inhibited during the reaction (see ESI, Fig. S6†), presumably leading to the improved total yield of products.

With optimized conditions in hand, the generality of the method was assessed (Scheme 1). 2-Substituted pyrenes **1** reacted with tertiary alkyl sulfones to give the corresponding mono- (**8a–11a**), and dialkylated products (**8aa–11aa**). In addition to alkylated PAHs, aryl- (**1b**), boryl- (**1c**) and silyl- (**1d**) substituted pyrene substrates were compatible with the reaction, leading to products incorporating these useful handles for further transformations. The exact structure of dialkylated product **8bb** was successfully confirmed by single-crystal X-ray diffraction analysis. Pyrenes bearing substituents at the 6-position yielded single products alkylated at the 8-position; the scope of alkylsulfones was thus investigated using pyrene derivative.[12] Tertiary alkyl sulfones that bear phenyl (**4c**) and silyloxy (**4d**) groups, which are easily prepared by α-alkylation, were converted into the desired products.

The mild basic conditions provide broad functional group compatibility. Sensitive functional groups such as cyano, alcohol, and bromo groups (**12e–12g**) were all tolerated. Cyclic tertiary alkyl groups with heteroatoms could be installed in good yields (**12h–12j**). Interestingly, the most bulky group examined, 3-ethyl-3-pentyl group (**12k**), did not give the desired product. Secondary alkyl substrates (**4l–4o**) also reacted smoothly under standard conditions, while primary alkylsulfones (**4p**, **4q**) showed lower reactivity. Benzyl, allyl, and methyl sulfones were not suitable (see ESI, Table S6†). Other 2,6-disubstituted pyrene derivatives (**13–16**) underwent alkylation with **4a** in moderate to good yields. Pyrenes conjugated with complex structures such as amino acids (**17r**) or steroids (**18s**) could be produced, which may be useful for biological applications.

Next, we subjected a variety of PAHs to alkylation with tertiary alkyl sulfones. The C3 position of fluoranthene (**19**) and perylene (**20**) were alkylated exclusively, affording mono-alkylated products. In the case of **20**, product yield was improved under green LED irradiation. It is worth noting that,

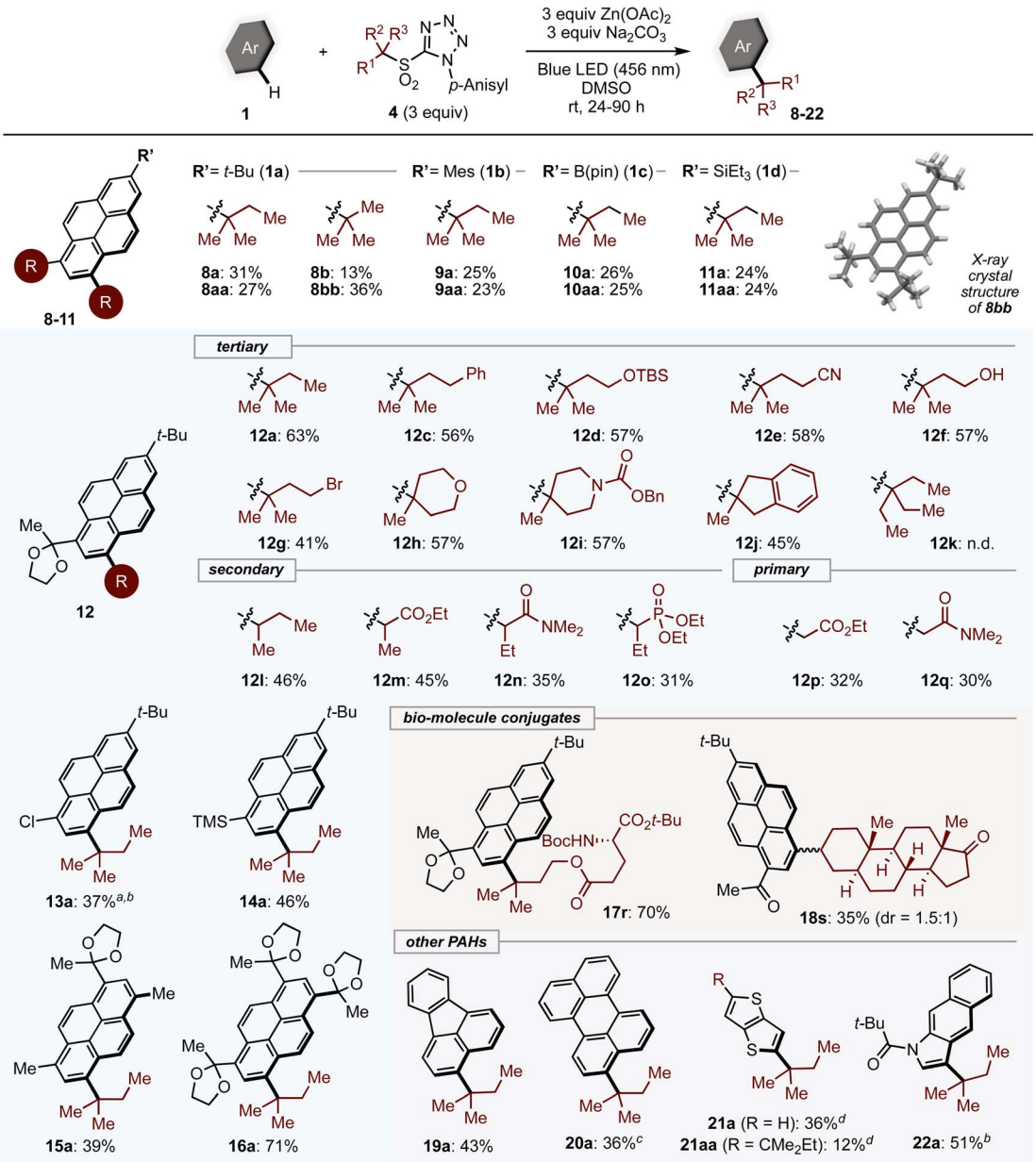

Scheme 1 Substrate scope. Isolated yields. Reaction conditions: PAH **1** (0.1–0.2 mmol), sulfone **4** (3 equiv.), $Zn(OAc)_2$ (3 equiv.), Na_2CO_3 (3 equiv.), DMSO (0.2 M), rt, 24–90 h. [a]5 equiv. sulfone was used. [b]without $Zn(OAc)_2$. [c]Green LED (525 nm) irradiation and *N*,*N*-dimethylformamide was used as a solvent. [d]Blue LED (427 nm) irradiation.

as with pyrene derivatives, the regioselectivity was different from that observed under Friedel–Crafts conditions.[30] PAHs containing heteroatoms such as thieno[3,2-*b*]thiophene (**21**) and benzo[*f*]indole (**22**) were also competent substrates. Unfortunately, small aromatics and highly π-extended PAHs were not applicable presumably due to weak absorption of visible light or a diminished reducing ability in the excited state (Table S6†).

The multiple C–H alkylation of pyrene (**23**) was also examined. To accomplish this, the low inherent solubility of pyrene was counteracted with excess sulfone **4d** and Na_2CO_3, and the reaction was cycled three times. Under these conditions, symmetric tetrasubstituted pyrene **23d** was obtained as a single regioisomer in 34% yield (Scheme 2).

The difference in regiospecificity compared with Friedel–Crafts alkylation suggests that the present photo-induced alkylation proceeds through a distinct reaction mechanism. To gain insight into the mechanism of this reaction, several control experiments were performed. Initially, we investigated the photoexcitation process. The UV-Vis absorption spectrum shows that pyrene **23** has almost no absorption in blue light region (>400 nm) at low concentration in DMSO solution (Fig. 3a). However, as the concentration is increased from 2 mM to 0.2 M, an absorption edge appears in the blue light region.

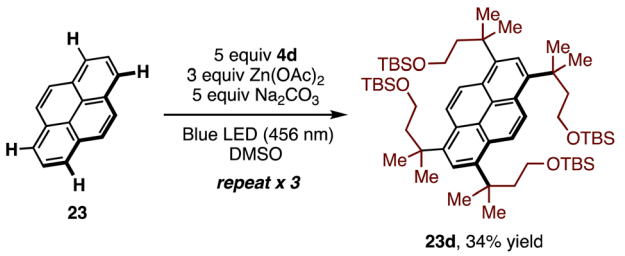

Scheme 2 Multiple C–H alkylation of pyrene with **4d**.

Similar phenomena were observed with other PAHs in concentrated solution (see ESI, Fig. S3†).

The red-shifting of the absorption wavelength can result from a PAH monomer at high concentration or aggregates resulting from stacking of PAHs,[31–33] which is essential for the photoexcitation of PAH substrates by blue LEDs. No absorption shift was observed in the solution of **23** with sulfone **4a**, thus an electron donor–acceptor complex between pyrene and sulfone is unlikely (see ESI, Fig. S4†). Stern–Volmer quenching studies conducted with **4a** reveal concentration-dependent quenching (Fig. 3b and c). The concentrated solution of pyrene exhibited a fluorescence maximum at 475 nm when excited by 390 nm light, which is derived from the excimer of pyrene. The quenching constants (k_q) at 2 mM and 0.2 M solution of **23** were determined to be 3.4×10^9 M^{-1} s^{-1} and 1.8×10^8 M^{-1} s^{-1}, respectively from the Stern–Volmer plot (see ESI, Fig. S9†) and the fluorescence lifetimes of the monomer ($\tau_0 = 230$ ns)[34] and excimer ($\tau_0 = 90$ ns).[35] These results suggest the SET process occurs from the lowest single excited state (S_1) of the pyrene monomer or dimer to the singlet ground state (S_0) of the alkylsulfone, resulting in the formation of pyrene monomer or dimer cation radicals and the sulfone anion radical.

To confirm the formation of cationic pyrene, we measured transient absorption spectra of pyrene in the presence of sulfone **4a** (Fig. 3d). The transient spectrum of pyrene (10 mM) and sulfone **4a** (200 mM) in DMSO at 100 ns is characterized by positive bands at 415, 445, 490 and 525 nm. The absorption peak at 445 nm is attributable to the radical cation of the pyrene monomer,[36] while the other peaks due to the triplet state vanished in the microsecond region. It should be noted that no absorption bands due to other species were observed, indicating that the decomposition of sulfone is negligible under these conditions, although the excitation wavelength of 355 nm is shorter than that used in Fig. 2a. In addition, the spectrum of a solution containing 200 mM of pyrene showed an increasing trend toward 400 nm together with disappearance of the 445 nm peak. This spectral signature is in line with an absorption band of the dimer cation of pyrene.[36] These results support the SET process as taking place between a pyrene monomer/dimer and sulfone.

A time-resolved electron spin resonance (TREPR) analysis also suggests the generation of radical species (Fig. 3e). The signal corresponding to the pyrene cation radical was confirmed, as reported for the intermolecular photoinduced

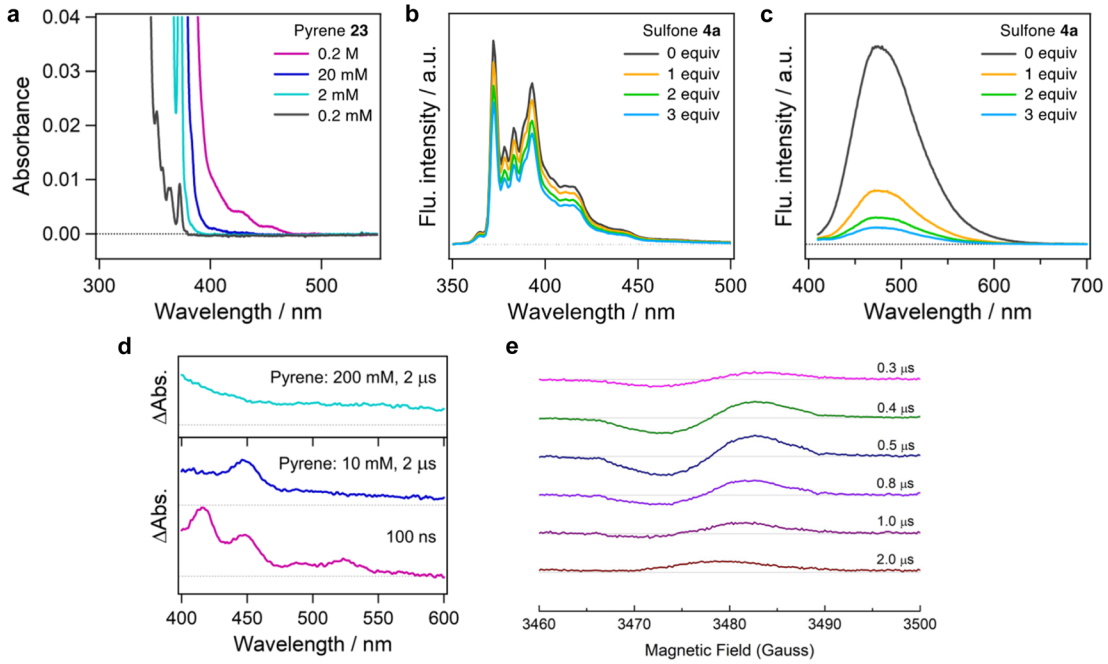

Fig. 3 Mechanistic investigations by spectroscopic analysis: (a) concentration-dependent UV-Vis absorption spectra of pyrene **23** in DMSO. (b) and (c) fluorescence quenching of **23** in DMSO (0.2 mM in DMSO, $\lambda_{ex} = 300$ nm, and 0.2 M in DMSO, $\lambda_{ex} = 390$ nm) by addition of sulfone **4a**. (d) Transient absorption spectra of **23** and **4a** in DMSO excited with a nanosecond laser pulse at 355 nm. Concentrations of **23** were respectively 0.2 M and 10 mM in the top and bottom panels. **4a** was dissolved at a concentration of 0.2 M in both the cases. (e) Delay time dependence of the time-resolved EPR spectrum. Concentrations of **23** and **4a** were 10 mM and 200 mM, respectively. The corresponding delay time is shown after a pulsed excitation light (wavelength: 355 nm, power: 2 mJ per pulse). EPR signal above or below the baseline corresponds to the microwave-absorption or microwave-emission, respectively.

charge-separation systems involving **23** (1 mM) and dicyanobenzene (10 mM).[37] The spin polarization pattern of emission/absorption in Fig. 3d denotes that the radical ion pair ($\mathbf{23}^{+\bullet}$ and $\mathbf{4a}^{-\bullet}$) generated by the charge-separation causes nuclear spin-state dependent electron spin polarization referred to as the radical pair mechanism (RPM)[38] through diffusive separation between the radicals in the presence of weak positive exchange interaction.[39]

Combined with spectroscopic evidence for radical generation, the overall photo-induced alkylation process was evaluated by density-functional theory (DFT) and time-dependent DFT (TD-DFT). The energy profile for the reaction of pyrene **23** with *tert*-butyl sulfone **24** is shown in Fig. 4a. Initially, **23** reaches its S_1 state (**23′**) from its S_0 state by vertical excitation, and then interacts with **24** to form intermediate **26**.

In **26**, the pyramidalization of the tetrazole carbon center indicates that the carbon should have anionic character. Natural population analysis (NPA) of **26** revealed that charge separation occurs between pyrene (total charge: +0.94) and sulfone (total charge: −0.94) (Fig. 4b). This is consistent with a spontaneous SET from **23′** to **24**, as supported by the results from spectroscopic analyses. The C(sp^3)–SO_2 bond of the metastable intermediate **27** was cleaved through a low activation energy ($\Delta G^{\ddagger}(\mathbf{TS_{27-28}})$ = 9.2 kcal mol^{-1}) path forming an excited-state complex between the tertiary carbon radical, the tetrazolyl sulfinate anion, and the pyrene cation (**28**).

Next, we assumed a radical coupling between the *tert*-butyl radical and pyrene radical cation in the S_1 state, but this pathway required high activation energies (see ESI, Fig. S11†). Therefore, the internal conversion from an S_1 state to an S_0 state likely takes place prior to C–C bond formation (from **27** to **28**). When the structure of **28** at the S_0 state was re-optimized, natural charge revealed that the positive charge was transferred from pyrene to the *tert*-butyl group, which supports a radical-polar crossover occurring to generate neutral pyrene and the *tert*-butyl cation (**29**). In the C–C bond forming process, the activation energy for the C1 pathway (red line, $\Delta G^{\ddagger}(\mathbf{TS_{29-30}})$ = 5.2 kcal mol^{-1}) was lower than that for the C2 pathway (blue line, $\Delta G^{\ddagger}(\mathbf{TS_{29-32}})$ = 9.7 kcal mol^{-1}), and the Gibbs reaction energy of cation intermediate **30** was more exergonic than that of **32**.[40] This indicates that the regioselectivity should be determined by the electron density of the highest occupied molecular orbital (HOMO) of pyrene rather than by steric factors. Deprotonation by Na_2CO_3 was largely downhill in both pathways, providing C1-alkylated product (**31**) exclusively. A similar energy profile was obtained through the formation of pyrene dimer (see ESI, Fig. S8†).

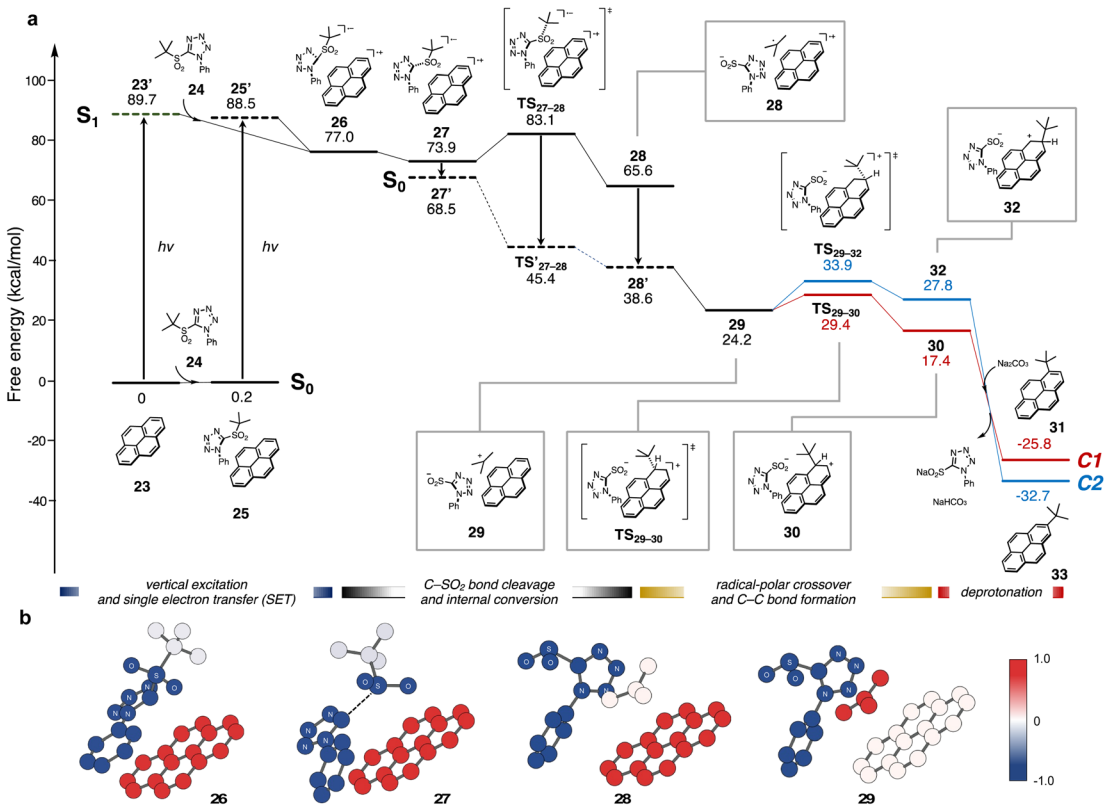

Fig. 4 Theoretical calculations: (a) energy profile for visible-light-induced direct C–H alkylation of **23** with *tert*-butyl sulfone **24**. Geometry optimizations of all structures in their ground state (S_0) were performed at CAM-B3LYP/6-31+G(d) level with IEFPCM solvation modeling (DMSO). With the optimized geometries, we performed thermal correction at 298.15 K and single point calculations to obtain the corresponding Gibbs free energy. Structures in the S_1 state were optimized at the TD-DFT level and the vertical S_0–S_1 excitation energy was also computed using the optimized S_0-state geometry. (b) Change of natural charge from S_0 equilibrium state (**25**) to each state. The whole charges of subgroups (*N*-phenyltetrazolyl sulfone, *tert*-butyl, and pyrene groups) were visualized.

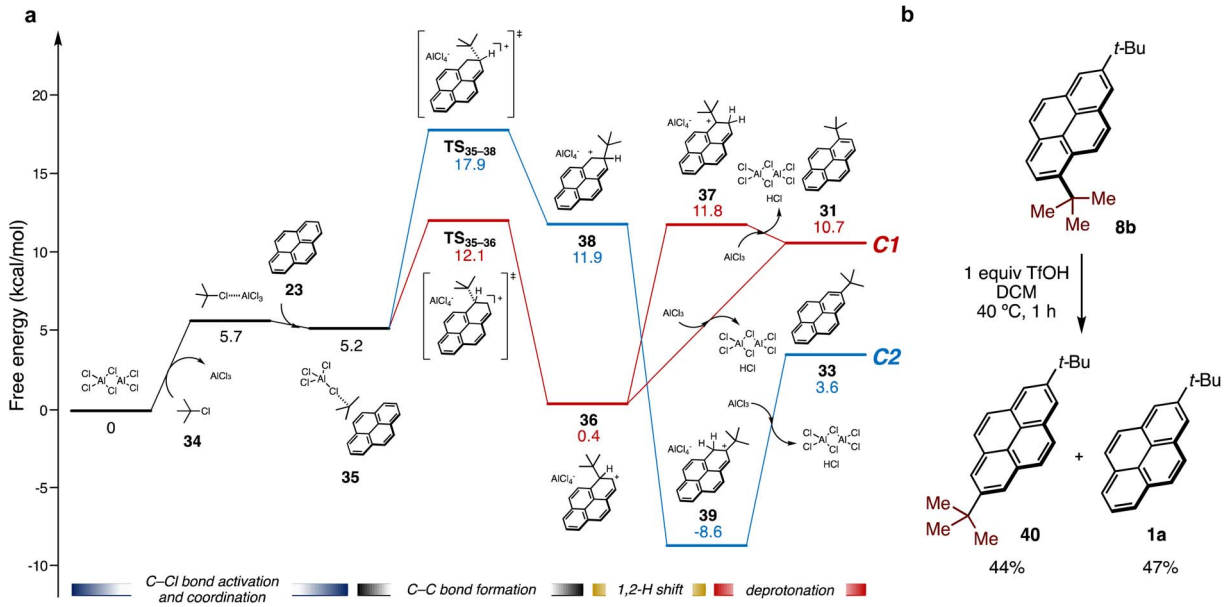

Fig. 5 Investigation of Friedel–Crafts alkylation: (a) energy profile for $AlCl_3$-mediated Friedel–Crafts alkylation of **23** with *tert*-butyl chloride **34** by DFT calculation. Gibbs free energies were calculated as in Fig. 4a with PCM solvation modeling (DCM). (b) The conversion of **8b** in the presence of trifluoromethanesulfonic acid (TfOH) in DCM. Yields were determined by GC analysis of the crude mixture using 1,3-dimethoxybenzene as an internal standard.

The mechanism for Friedel–Crafts alkylation of pyrene **23** with *tert*-butyl chloride (**34**) promoted by $AlCl_3$ as a Lewis acid was also computed to evaluate regiospecificity (Fig. 5a). $AlCl_3$ exists as complicated Cl-bridged polymeric structures in the solid state, thus a simplified dimeric structure (Al_2Cl_6) was employed. The Friedel–Crafts alkylation should proceed through following steps: activation of **34** by coordination of $AlCl_3$, electrophilic attack on **23**, and then deprotonative rearomatization to form an alkylated pyrene with HCl loss and regeneration of Al_2Cl_6. As with the photo-induced reaction, the activation energy for the C1 pathway (red line, $\Delta G^{\ddagger}(\mathbf{TS_{35-36}})$) is lower than that for the C2 pathway (blue line, $\Delta G^{\ddagger}(\mathbf{TS_{35-38}})$) (12.1 kcal mol^{-1}, 17.9 kcal mol^{-1}, respectively). However, the deprotonation of intermediate **36** to afford **31** is energetically uphill. On the other hand, intermediate **38** can be converted by a 1,2-proton shift to tertiary carbocationic intermediate **39**, which is even more stable than **33** formed by deprotonation.

The formation of a similar carbocation intermediate (**37**) from **36** by a 1,2-proton shift was also unfavorable, probably due to the steric repulsion between the *tert*-butyl group and the hydrogen atom. Therefore, **36** preferentially reverts to **38** by reversible C–C bond formation under acidic conditions to form **39**, resulting in exclusive formation of C2 product **33** after neutralization. Indeed, under experimental conditions, 1,7-di-*tert*-butylpyrene (**8b**) was rapidly converted into 2,7-di-*tert*-butylpyrene **40** and **1a** in 44% and 47% GC yields, respectively, by treatment of stoichiometric amount of trifluoromethanesulfonic acid (TfOH) (Fig. 5b). This result clearly demonstrates formal rearrangement from the kinetically stable C1 product to the thermodynamically stable C2 product promoted by acid, which is consistent with the results from DFT calculations.

Conclusions

We have shown that the intrinsic photochemical properties of PAHs can promote a regiospecific C–H alkylation of PAHs without the need for separate photocatalysts or any type of catalysis. Based on all theoretical calculations, it is noteworthy that even though both reactions proceed through similar carbocationic intermediates, the regioselectivity changes depend completely on whether the reactions are under acidic or basic conditions rather than steric factors. The present photo-triggered process enables the generation of carbocations under basic conditions through a single electron shuttle between the PAH and the alkylating agent, providing kinetically favored products though thermodynamically disfavored intermediates by shunting acid-catalyzed isomerization pathways. This approach overcomes the substrate limitations of thermal reaction conditions, opening up a new avenue for the facile preparation of unexplored PAH-based functional materials, and highlighting the utility of organosulfones as redox-active substrates in organic synthesis.

Data availability

All experimental data and computational data are available in the ESI.†

Author contributions

C. M. C. and M. N. conceived the concept and supervised the project. M. O., K. G., and J. C.-H. Y. developed the reactions and performed and analyzed experiments. H. S. and H. M. performed transient absorption analysis. T. O. and Y. K. performed

time-resolved EPR analysis. K. S., D. Y., and M. N. performed the DFT calculation. H. S., Y. K., D. Y., H. M., C. M. C., and M. N. wrote the manuscript with assistance from co-authors.

Conflicts of interest

The authors declare no conflicts of interest.

Acknowledgements

We thank Dr Yoshitaka Aramaki (Nagoya University) for assistance with X-ray crystal-structure analysis. This work is supported by Japan Society for the Promotion of Science (JSPS) (JP21H01888, JP21H05395, JP23H03956, JP23H04877 (H. S.), JP22H00344, JP20H05835 (Y. K.), JP21H01889, JP21K18934 (H. M.), JPMJPR21C9 (D. Y.), JP21K05068, JP21H05390 (M. N.)), Kansai Research Foundation for Technology Promotion (H. S.), Japan Science and Technology Agency (JST-CREST) (JPMJCR23I6 (Y. K.)). We acknowledge JSPS and Nagoya University through The World Premier International Research Centre Initiative (WPI) program. We thank the support from The Natural Sciences and Engineering Research Council of Canada (NSERC) (RGPIN/04667-2016) (C. M. C.), and the Canada Foundation for Innovation (CFI) (33355) (C. M. C.). We also thank Dr Jean Bouffard (Ewha Womans University) and Dr Issey Takahashi (Nagoya University) for helpful discussions and suggestions.

Notes and references

1 A. Kekulé, *Bull. Soc. Chim. Fr.*, 1865, **3**, 98.
2 L. T. Scott, *Angew. Chem., Int. Ed.*, 2004, **43**, 4994.
3 I. A. Stepek, M. Nagase, A. Yagi and K. Itami, *Tetrahedron*, 2022, **123**, 132907.
4 H. Beck, M. Härter, B. Haß, C. Schmeck and L. Baerfacker, *Drug Discovery Today*, 2022, **27**, 1560.
5 J. Hou, O. Inganas, R. H. Friend and F. Gao, *Nat. Mater.*, 2018, **17**, 119.
6 G. Hong, X. Gan, C. Leonhardt, Z. Zhang, J. Seibert, J. M. Busch and S. Bräse, *Adv. Mater.*, 2021, **33**, e2005630.
7 N. Panwar, A. M. Soehartono, K. K. Chan, S. Zeng, G. Xu, J. Qu, P. Coquet, K. T. Yong and X. Chen, *Chem. Rev.*, 2019, **119**, 9559.
8 Y. Gu, Z. Qiu and K. Müllen, *J. Am. Chem. Soc.*, 2022, **144**, 11499.
9 H. Ito, Y. Segawa, K. Murakami and K. Itami, *J. Am. Chem. Soc.*, 2019, **141**, 3.
10 M. Grzybowski, B. Sadowski, H. Butenschon and D. T. Gryko, *Angew. Chem., Int. Ed.*, 2020, **59**, 2998.
11 A. Borissov, Y. K. Maurya, L. Moshniaha, W. S. Wong, M. Żyła-Karwowska and M. Stępień, *Chem. Rev.*, 2022, **122**, 565.
12 F. Würthner, C. R. Saha-Moller, B. Fimmel, S. Ogi, P. Leowanawat and D. Schmidt, *Chem. Rev.*, 2016, **116**, 962.
13 K. Kawasumi, Q. Zhang, Y. Segawa, L. T. Scott and K. Itami, *Nat. Chem.*, 2013, **5**, 739.
14 A. K. Pal, C. Li, G. S. Hanan and E. Zysman-Colman, *Angew. Chem., Int. Ed.*, 2018, **57**, 8027.
15 M. Fukazawa, F. Takahashi and H. Yorimitsu, *Org. Lett.*, 2021, **23**, 4613.
16 P. H. Gore, *Chem. Rev.*, 1955, **55**, 229.
17 L. Rodenburg, R. Brandsma, C. Tintel, J. Van Thujil, J. Lugtenburg and J. Cornelisse, *Recl. Trav. Chim. Pays-Bas*, 1986, **105**, 156.
18 A. Wrona-Piotrowicz, A. Makal and J. Zakrzewski, *J. Org. Chem.*, 2020, **85**, 11134.
19 D. N. Coventry, A. S. Batsanov, A. E. Goeta, J. A. K. Howard, T. B. Marder and R. N. Perutz, *Chem. Commun.*, 2005, 2172.
20 P. E. Hansen, A. Berg and H. Lund, *Acta Chem. Scand., Ser. B*, 1976, **30**, 267.
21 B. M. Trost and C. A. Kalnmals, *Chem.–Eur. J.*, 2019, **25**, 11193.
22 M. Nambo, Y. Maekawa and C. M. Crudden, *ACS Catal.*, 2022, **12**, 3013.
23 J. Corpas, S. H. Kim-Lee, P. Mauleón, R. G. Arrayás and J. C. Carretero, *Chem. Soc. Rev.*, 2022, **51**, 6774.
24 M. Nambo, Y. Tahara, J. C.-H. Yim, D. Yokogawa and C. M. Crudden, *Chem. Sci.*, 2021, **12**, 4866.
25 T. Sengoku, D. Ogawa, H. Iwama, T. Inuzuka and H. Yoda, *Chem. Commun.*, 2021, **57**, 9858.
26 Q. Wang, B. C. Lee, T. J. Tan, Y. Jiang, W. H. Ser and M. J. Koh, *Nat. Synth.*, 2022, **1**, 967.
27 M. Nambo, K. Ghosh, J. C.-H. Yim, Y. Tahara, N. Inai, T. Yanai and C. M. Crudden, *ACS Catal.*, 2022, **12**, 9526.
28 S. Patel, B. Paul, H. Paul, R. Shankhdhar and I. Chatterjee, *Chem. Commun.*, 2022, **58**, 4857.
29 S. Murarka, *Adv. Synth. Catal.*, 2018, **360**, 1735.
30 L. B. A. Johansson, J. G. Molotkovsky and L. D. Bergelson, *J. Am. Chem. Soc.*, 1987, **109**, 7374.
31 N. Mataga, Y. Torihashi and Y. Ota, *Chem. Phys. Lett.*, 1967, **1**, 385.
32 A. Itaya, T. Kawamura, H. Masuhara, Y. Taniguchi, M. Mitsuya, H. Uraki, K. Kano and S. Hashimoto, *Chem. Lett.*, 1986, **15**, 1541.
33 F. Ito, S. Miyadera, H. Matsuda, Y. Ishibashi, S. Ito and H. Miyasaka, *Photochem. Photobiol. Sci.*, 2018, **17**, 910.
34 A. Nakajima, *Bull. Chem. Soc. Jpn.*, 1973, **46**, 2602.
35 J. B. Birks, D. J. Dyson and I. H. Munro, *Proc. R. Soc. London, Ser. A*, 1963, **275**, 575.
36 A. Kira, S. Arai and M. Imamura, *J. Chem. Phys.*, 1971, **54**, 4890.
37 S. N. Batchelor, H. Heikkila, C. W. M. Kay, K. A. Mclauchlan and I. A. Shkrob, *Chem. Phys.*, 1992, **162**, 29.
38 F. J. Adrian, *Rev. Chem. Intermed.*, 1979, **3**, 3.
39 Y. Kobori, S. Sekiguchi, K. Akiyama and S. Tero-Kubota, *J. Phys. Chem. A*, 1999, **103**, 5416.
40 M. J. S. Dewar and R. D. Dennington, *J. Am. Chem. Soc.*, 1989, **111**, 3804.